PHYSICAL REVIEW A **80**, 041804(R) (2009)

Self-alignment and instability of waveguides induced by optical forces

Amit Mizrahi,* Kazuhiro Ikeda, Fabio Bonomelli, Vitaliy Lomakin, and Yeshaiahu Fainman
Department of Electrical and Computer Engineering, University of California–San Diego, 9500 Gilman Drive, La Jolla, California 92093-0407, USA

(Received 8 April 2009; published 9 October 2009)

We introduce a fundamental property of waveguides induced by the forces of the guided light, namely, the ability to self-align or be in instability. A nanoscale waveguide broken by an offset and a gap may tend to self-align to form a continuous waveguide. Conversely, depending on the geometry and light polarization, the two parts of the waveguide may be deflected away from each other, thus, being in an unstable state. These effects are unique as they rely on the presence of both the guided mode and the scattered light. Strong self-alignment forces, in both the transverse and longitudinal directions, may be facilitated by near field interaction with polarization surface charges.

DOI: 10.1103/PhysRevA.80.041804 PACS number(s): 42.50.Wk, 03.50.De, 42.25.Bs

Laser light has significant mechanical effects on microscopic objects, as was initially pointed out about four decades ago [1]. In addition to the vast work on trapping and manipulation of small particles [2], much effort has been directed at cavity-based optomechanical devices, where optical forces may be considerably enhanced [3–5]. A less explored option, however, is optical forces on waveguides, which become observable at the microscopic scale [6,7].

Research of optical forces on waveguides is motivated by the growing capabilities of nanofabrication that enable new possibilities of nanoscale light manipulation [8–10]. The theory of guided light is thus being extended to include the laws of the mechanical effects of light on the guiding structure itself [11–16]. These new physical mechanisms relate the properties of the guided modes to the forces created by them. For instance, light guided between two waveguides or mirrors creates a repulsive force for an antisymmetric transverse field and an attractive force for a symmetric transverse field [12,13]. Moreover, a superposition of a symmetric and antisymmetric modes may hold the waveguide in a stable equilibrium [13,15,17]. Such phenomena can be experimentally observed in nanomechanical devices fabricated on a chip, as was recently demonstrated with a suspended silicon waveguide [18].

In this Rapid Communication, we introduce a fundamental property of waveguides, namely, the ability of a waveguide to self-align by light forces when it is perturbed by a small offset misalignment. We show that the size of the waveguide and the type of eigenmode determine whether the two misaligned parts will tend to self-align or deflect away from each other. This phenomenon is unique as it relies on both the *guided* waveguide eigenmode and the *scattered* radiation from the perturbation. A strong self-alignment force is created due to polarization surface charges that dominate the optical force with a near field interaction. We further investigate the exerted forces when a gap is introduced between the two parts of the waveguide.

The geometry under consideration is shown in Fig. 1. A single mode slab waveguide of half-width d and permittivity ε_r is broken by an offset in the x axis Δ and a gap in the z axis g. An eigenmode is incident from the left (input waveguide) carrying power P_{in}, most of which is transmitted to the output waveguide (P_{out}), while the remainder is either scattered (P_{sca}) or reflected back into the input waveguide. No variations in the geometry are assumed along the y axis, and, therefore, all quantities given are per unit length.

First, we examine the case of no gap $g=0$ and a small offset Δ. For the calculation of the fields, we take an approach of mode matching approximation, similar to that described by Marcuse [19,20]. We begin by considering a transverse electric (TE) incident mode, for which the nonzero field components are E_y, H_x, and H_z. The even guided mode incident from the left is given inside the dielectric slab by $E_i = A_{TE}\cos(k_x x)\exp(-j\beta_g z)$, where $A_{TE} = \sqrt{2\omega\mu_0 P_{in}/\beta_g(d+\gamma^{-1})}$, k_x is the transverse wave number in the dielectric, β_g is the longitudinal wave number, γ is the transverse decay constant outside the slab, and the time dependence is of the form $e^{j\omega t}$. The transverse electric field in each region may be represented as a sum of the guided modes and the continuous spectrum of the radiation modes (Ref. [20], pp. 314–319), corresponding to the scattered light. Explicitly, assuming the interface plane is at $z=0$, then for $z<0$ (input waveguide) this field is given by

$$E_1 = E_i + a_r E_r + \int_0^\infty d\rho q_{e1}(\rho)E_{e1} + \int_0^\infty d\rho q_{o1}(\rho)E_{o1}, \quad (1)$$

whereas for $z>0$ (output waveguide) it reads as

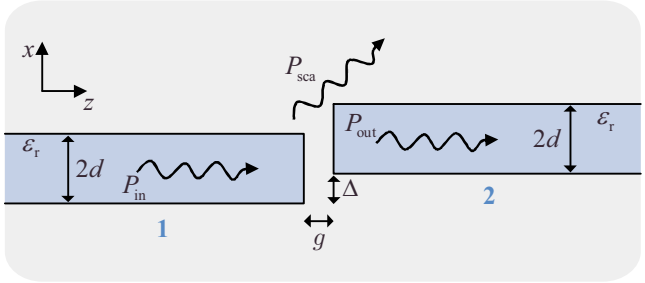

FIG. 1. (Color online) A single mode slab waveguide broken by an offset and a gap.

*amitmiz@ece.ucsd.edu

 ©2009 The American Physical Society

$$E_2 = a_t E_t + \int_0^\infty d\rho q_{e2}(\rho) E_{e2} + \int_0^\infty d\rho q_{o2}(\rho) E_{o2}. \quad (2)$$

In the above two equations, a_r and a_t are the reflection and transmission coefficients of the guided mode, respectively; E_r and E_t are the reflected and transmitted guided modes, respectively; $q_{e1,2}$ and $q_{o1,2}$ are the amplitudes of the even and odd radiation modes, respectively; $\rho = \sqrt{k_0^2 - \beta_r^2}$ is the transverse wave number of the radiation modes outside the slabs, where β_r is their longitudinal wave number and $k_0 = \omega/c$; $E_{e1,2}$ and $E_{o1,2}$ are the even and odd radiation modes, respectively. The amplitudes of the guided and the radiation modes may be approximated analytically by expressions containing the overlap integral of the type of Eq. (9.5-10) in Ref. [20] between the respective mode and the incident guided mode.

Generally, force densities on dielectrics may be viewed as resulting from two processes involving the polarization density $\vec{P} = \varepsilon_0(\varepsilon_r - 1)\vec{E}$ [13,21–23]: (i) time-averaged interaction of effective polarization *volume* current densities with the magnetic field $\frac{1}{2}\mathrm{Re}(j\omega\vec{P} \times \mu_0\vec{H}^*)$ and (ii) the interaction of polarization *surface* charge densities with the electric field $\frac{1}{2}\mathrm{Re}[(\hat{n}\cdot\vec{P})\vec{E}^*]$, where $\hat{n}$ is the normal to the surface of the dielectric. In the TE case, no surface charge densities are formed, and, thus, the volume force density in the x direction is integrated and obtained in terms of integration over only the top and bottom surfaces

$$F_{x2} = \frac{1}{4}\varepsilon_0(\varepsilon_r - 1)\int_0^\infty dz(|E_2|^2|_{x=d+\Delta} - |E_2|^2|_{x=-d+\Delta}). \quad (3)$$

Once an offset ($\Delta \neq 0$) is introduced, symmetry is broken, and scattering occurs from the discontinuity giving rise to a transverse force.

For the evaluation of the force on the output waveguide, the field expression of Eq. (2) is substituted into Eq. (3). At this point, we are interested in small offsets, so that only terms up to the first order of Δ are kept. Noting that cross-products of the even radiation modes with the odd radiation modes are of order larger than Δ, and using the symmetry properties of the modes, the expression for the force reads as

$$F_{x2} \simeq \varepsilon_0(\varepsilon_r - 1)\mathrm{Re}\int_0^\infty dz E_t^* \int_0^\infty d\rho q_{o2}(\rho) E_{o2}, \quad (4)$$

where the integration is performed at $x = d + \Delta$. Hence, it is evident that the odd radiation modes created by the scattering are responsible for the transverse force on the waveguide. A direct measure of the waveguide's tendency to move either way is the derivative of the force with respect to Δ, $dF_{x2}/d\Delta(\Delta = 0)$ denoted by F'_{x2}. Bearing in mind that $F_{x2}(\Delta = 0) = 0$, the force may be approximated by $F'_{x2}\Delta$. The only term in the above equation that depends on Δ is q_{o2}, and an analytic expression for $dq_{o2}/d\Delta$ may be obtained. The integration over z is then performed analytically, and the closed-form expression for the derivative reads

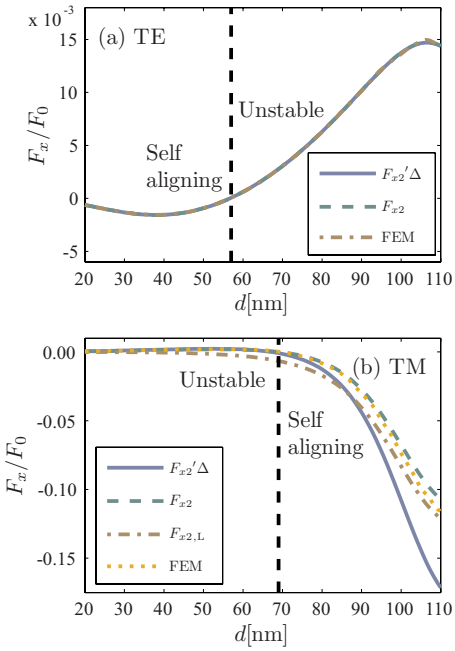

FIG. 2. (Color online) Transverse force as a function of d for an offset Δ of 2% of d. The permittivity of the waveguides is $\varepsilon_r = 3.48^2$, and the wavelength is $\lambda = 1.55$ μm. (a) TE incident mode. (b) TM incident mode.

$$F'_{x2} = \varepsilon_0(\varepsilon_r - 1)^2 k_0^2 A_{TE}^2 \cos^2(k_x d)/\pi \int_0^\infty d\rho \times \frac{1}{1 + \frac{\sigma^2}{\rho^2}\cot^2(\sigma d)} \frac{1}{\gamma^2 + \rho^2} \mathrm{Re}\left[\frac{j(\beta_r + \beta_g)}{\beta_r(\beta_r - \beta_g)}\right], \quad (5)$$

where $\sigma = \sqrt{\varepsilon_r k_0^2 - \beta_r^2}$ is the radiation modes transverse wave number inside the slab. While the spectrum of radiation modes contains both propagating modes having real β_r (where $\rho < k_0$) and evanescent modes having imaginary β_r (where $\rho > k_0$), the expression in the square brackets is purely imaginary for the propagating modes, so that it is only the evanescent radiation modes that contribute to the generation of this force.

Both the force F_{x2} [Eq. (4)] and the quantity $F'_{x2}\Delta$ [Eq. (5)] are plotted in Fig. 2(a) as a function of d, for an offset of 2% of d. The range of d shown is 20–110 nm, where the slab is single mode in each polarization. The wavelength is taken to be $\lambda = 1.55$ μm and the permittivity is 3.48^2, corresponding to silicon at that wavelength. The forces are normalized by $F_0 \equiv P_{in}/c$, which is the momentum per unit time carried by a plane wave. These results are compared with a finite element method (FEM) simulation, and as seen the three curves are virtually identical. In addition to the integration of the force on the polarization densities, all results were validated by integration over the Maxwell stress tensor [21] with excellent agreement.

The plot of Fig. 2(a) reveals two regimes; the first is a self-alignment regime up to a slab half-width of about 57 nm, for which $F'_{x2} < 0$ corresponding to a restoring force. The

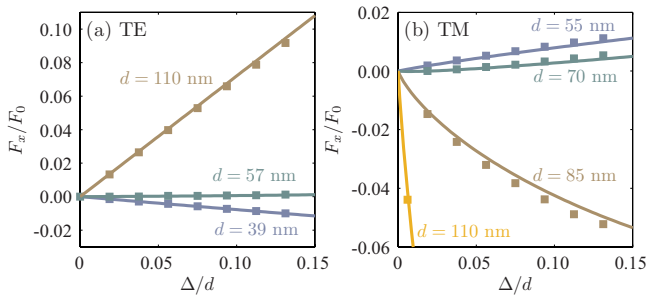

FIG. 3. (Color online) Transverse force F_{x2} as a function of the offset Δ for different values of waveguide half-width d. The solid line corresponds to the analytic analysis and the square markers indicate FEM simulation results. (a) TE incident mode. (b) TM incident mode.

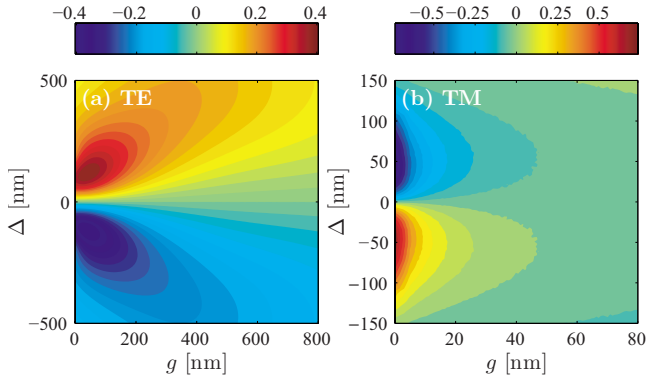

FIG. 4. (Color online) Contours of F_{x2}/F_0 as a function of g and Δ for d=110 nm and ε_r=3.48^2. (a) TE incident mode. (b) TM incident mode.

second is an instability regime in which a small offset results in a deflection force. Although we show here only the transverse force on the output waveguide, when the offset is small, the scattered power is negligible and by virtue of momentum conservation, the force on the input waveguide is of the same magnitude and opposite in sign to that on the output waveguide. In fact, we have shown analytically that $F'_{x1}=-F'_{x2}$. To better illustrate the different regimes, we depict in Fig. 3(a) the transverse force F_{x2} as a function of Δ for d=39 nm where a negative restoring force is seen, d=57 nm where the force derivative at Δ=0 vanishes at the transition between the two regimes, and for d=110 nm where instability in the form of a deflecting force is observed.

When the incident mode is transverse magnetic (TM), the situation is considerably more involved. The field components for the TM mode are E_x, E_z, and H_y, and the incident magnetic field is given by $H_i=A_{TM}\cos(k_x x)\exp(-j\beta_g z)$ [20]. The fields in each region are described by Eqs. (1) and (2) with E replaced by H. The force mechanism in the TM case differs substantially than that of the TE case, as for the TM the electric field has normal components to the discontinuities in the dielectric, and therefore polarization surface charge densities are formed. Considering again the output waveguide, the first contribution is from the polarization surface charge densities created by E_z at the z=0 interface. The force density of this term is given by $\frac{1}{2}\mathrm{Re}[-\varepsilon_0(\varepsilon_r-1)E_z E_x^*]$, where E_z is the field just inside the slab at z=0. Calculation of this force on the output waveguide while keeping only terms up to the first order of Δ yields

$$F_{x2,L} \simeq \frac{A_{TM}}{2}\frac{\varepsilon_0(\varepsilon_r-1)}{(\omega\varepsilon_0\varepsilon_r)^2}\mathrm{Re}\, j\int_0^\infty d\rho q_{o2}(\rho) \times\left\{\frac{(k_x\beta_r+\sigma\beta_g)\sin[(k_x-\sigma)d]}{(k_x-\sigma)} - \frac{(k_x\beta_r-\sigma\beta_g)\sin[(k_x+\sigma)d]}{(k_x+\sigma)}\right\}, \quad (6)$$

where an analytic expression for q_{o2} may be obtained. The two other contributions, for which we do not present here the closed-form expressions, are from the polarization surface charge densities formed on the top and bottom surfaces of the waveguide and from the polarization volume current density. As shown below, these two contributions are subdominant in the region of interest. Similarly to the TE mode, only the evanescent part of the odd radiation mode spectrum participates in the generation of the force as the expression in the curly brackets, as well as q_{o2}, is purely real for $\rho<k_0$. The relation $F'_{x1}=-F'_{x2}$ holds for the TM case as well.

The quantities $F'_{x2}\Delta$, F_{x2}, as well as the force calculated by FEM, are shown in Fig. 2(b) as a function of d for an offset Δ of 2%. Contrary to the TE case, here instability occurs for small values of d, and above about 70 nm there is self-alignment. The instability peak force for the TM is weaker by about an order of magnitude than that of the TE. The restoring force, however, increases monotonically, so that at the maximum value in the shown range of d, it is about two orders of magnitude stronger than the peak value of the TE restoring force. This dramatic difference is due to the presence of electric field components that are perpendicular to the dielectric boundaries. Specifically, at the left boundary of the output waveguide (z=0 plane), E_z induces a polarization surface charge density, while E_x gives it a transverse kick. The result $F_{x2,L}$ given by Eq. (6) is plotted in Fig. 2(b). This force is negative for the entire range of d and is seen to comprise almost all of the total force in the self-alignment regime. Qualitatively, it may be associated with a dipole induced by the guided mode, which has $E_z\propto\sin(k_x d)$, and the strength of the dipole per power increases with d as the mode confinement increases. At the z=0 interface, the dipole is roughly inverted, and, consequently, the two parts attract each other, in both the transverse and longitudinal directions. Moreover, this force grows rapidly as a function of Δ and is therefore responsible for the derivative approximation being less accurate than for the TE case. This is seen in Fig. 3(b), where F_{x2} is plotted for four different values of d: d=55 nm where instability is observed, d=70 nm about where the derivative vanishes at Δ=0, d=85 nm which exhibits self-alignment, and d=110 nm, where there is strong self-alignment which is further discussed below.

We next extend the discussion by introducing a longitudinal gap $g\neq 0$. Figures 4(a) and 4(b) show contours of F_{x2} in the $g-\Delta$ plane obtained by FEM simulations, for TE and TM incident modes, respectively. The slab half-width is assumed

to be $d=110$ nm, where according to Fig. 2, the TE mode places the system in instability, whereas the TM mode causes self-alignment. In both cases, the $g=0$ behavior extends to larger values of g, but the decay of the TE repulsive force with the offset and gap is much slower than that of the attractive TM force, as seen by the scales of g and Δ of the two frames of Fig. 2. The maximum TE force is about $0.4F_0$ and it is obtained for about $\Delta \simeq 130$ nm and $g \simeq 50$ nm. A waveguide cantilever at $\Delta=0$ is, in fact, in a bistable state, where a small offset may result in a deflection force that would eventually be balanced by the mechanical force. The maximum attractive TM force is obtained for $g=0$ and $\Delta \simeq 45$ nm, and it is about $0.7F_0$. We further found that a strong longitudinal force, facilitated mainly by the E_z dipoles at the two facets, is pulling the two waveguides toward each other at a force of about $2F_0$ for $g \simeq 20$ nm. For large enough values of g, the TM force becomes repulsive, corresponding to radiation pressure.

The self-alignment and instability may be tested experimentally by fabricating on a chip two waveguide cantilevers with an offset and a gap. For instance, taking a length in the y direction Δ_y, then for $P_{\text{in}}\Delta_y=30$ mW, $F_0\Delta_y=100$ pN, and at $\Delta \simeq 50$ nm and $g=20$ nm, we obtain $F_{x2}\Delta_y \simeq -0.1F_0\Delta_y$ according to Fig. 2(b), which is about 10 pN. This is on the order of magnitude of force that was shown in Ref. [18] to actuate a silicon suspended waveguide, and similarly the thermal effects are expected to be insignificant compared to the optical forces. Three-dimensional FEM simulations show that for the fundamental mode of a rectangular waveguide 400 nm wide and 200 nm thick, the maximum force is enhanced, so that at $g=20$ nm, it is about $-0.3F_0$ obtained at $\Delta \simeq 100$ nm. The deflection of the waveguide in such a system may be viewed by the nonlinear input-output behavior, as the output power increases when the cantilevers tend to self-align. The cantilevers may also be vibrated at their mechanical resonance by modulating the incident power, resulting in a system that may be suitable for applications such as sensing.

In conclusion, we demonstrated an effect of light forces in the form of self-alignment or instability of a waveguide broken by an offset and a gap. The waveguide size and mode polarization determine which of the two regimes the waveguide is in. Closed-form expressions for the transverse forces were given for the case of a small offset and no gap. The forces described here are unique as they are due to the presence of both the guided mode and the scattered light from the discontinuity. Strong self-alignment in both dimensions for a TM mode is caused by near field interaction of the polarization surface charges created by the longitudinal electric field. The effects presented here suggest a way for holding a cantilever in a stable equilibrium as well as vibrating it, with applications in light-driven machines, and specifically in sensing.

This work was supported by the Defense Advanced Research Projects Agency, the National Science Foundation, the NSF CIAN ERC, the U.S. Air Force Office of Scientific Research, the U.S. Army Research Office, and the Technion Viterbi Family Foundation.

[1] A. Ashkin, Phys. Rev. Lett. **24**, 156 (1970).
[2] D. G. Grier, Nature (London) **424**, 810 (2003).
[3] M. Notomi, H. Taniyama, S. Mitsugi, and E. Kuramochi, Phys. Rev. Lett. **97**, 023903 (2006).
[4] T. J. Kippenberg and K. J. Vahala, Science **321**, 1172 (2008).
[5] M. Tomes and T. Carmon, Phys. Rev. Lett. **102**, 113601 (2009).
[6] M. Eichenfield, C. P. Michael, R. Perahia, and O. Painter, Nat. Photonics **1**, 416 (2007).
[7] W. She, J. Yu, and R. Feng, Phys. Rev. Lett. **101**, 243601 (2008).
[8] Q. Xu, V. R. Almeida, R. R. Panepucci, and M. Lipson, Opt. Lett. **29**, 1626 (2004).
[9] U. Levy, M. Abashin, K. Ikeda, A. Krishnamoorthy, J. Cunningham, and Y. Fainman, Phys. Rev. Lett. **98**, 243901 (2007).
[10] D. T. H. Tan, K. Ikeda, R. E. Saperstein, B. Slutsky, and Y. Fainman, Opt. Lett. **33**, 3013 (2008).
[11] M. L. Povinelli, M. Ibanescu, S. G. Johnson, and J. D. Joannopoulos, Appl. Phys. Lett. **85**, 1466 (2004).
[12] M. L. Povinelli, M. Lončar, M. Ibanescu, E. J. Smythe, S. G. Johnson, F. Capasso, and J. D. Joannopoulos, Opt. Lett. **30**, 3042 (2005).
[13] A. Mizrahi and L. Schächter, Opt. Express **13**, 9804 (2005).
[14] A. Mizrahi and L. Schächter, Phys. Rev. E **74**, 036504 (2006).
[15] A. Mizrahi and L. Schächter, Opt. Lett. **32**, 692 (2007).
[16] A. Mizrahi, M. Horowitz, and L. Schächter, Phys. Rev. A **78**, 023802 (2008).
[17] P. T. Rakich, M. A. Popović, M. Soljačić, and E. P. Ippen, Nat. Photonics **1**, 658 (2007).
[18] M. Li, W. H. P. Pernice, C. Xiong, T. Baehr-Jones, M. Hochberg, and H. X. Tang, Nature (London) **456**, 480 (2008).
[19] D. Marcuse, Bell Syst. Tech. J. **49**, 273 (1970).
[20] D. Marcuse, *Light Transmission Optics* (Van Nostrand, New York, 1972).
[21] J. Schwinger, L. L. DeRadd, K. A. Milton, and W.-Y. Tsai, *Classical Electrodynamics* (Perseus Books, Reading, MA, 1998).
[22] M. Mansuripur, Opt. Express **12**, 5375 (2004).
[23] B. A. Kemp, T. M. Grzegorczyk, and J. A. Kong, Phys. Rev. Lett. **97**, 133902 (2006).